

# A new strategy to reduce amyloid deposition using peptide-imprinted membranes

Caterina Cristallini<sup>1</sup>, Elena Bellotti<sup>2</sup>, Francesca Spezia<sup>2</sup>, Elisabetta Rosellini<sup>2</sup>, Maria G. Cascone<sup>2</sup>, Niccoletta Barbani<sup>2</sup>

<sup>1</sup>CNR Institute for Polymers, Composites and Biomaterials, UOS Pisa, Pisa - Italy

<sup>2</sup>Department of Civil and Industrial Engineering, University of Pisa, Pisa - Italy

## ABSTRACT

**Background:** The accumulation of amyloid beta protein in the brain causes the cognitive impairment observed in neurodegenerative pathologies such as Alzheimer's disease. The present study aimed to test the hypothesis that a rapid removal of amyloid beta protein peptides from the blood by an extracorporeal purification system could represent an alternative solution for the treatment of patients suffering from this neurodegenerative disease.

**Methods:** In this regard, we investigated the specific recognition properties of a molecularly imprinted membrane based on poly(ethylene-co-vinyl alcohol) toward the amyloid beta protein fragment 25-35 (AbP), the more neurotoxic domain of amyloid beta protein. A chemical modification of the copolymer backbone using succinic anhydride was also performed to favor the formation of carboxylic groups and thus improve imprinting performance.

**Results:** The physico-chemical, morphological, mechanical and functional characterisations gave interesting results confirming the ability of imprinted membranes to *in vitro* rebind AbP.

**Conclusions:** This work represents a proof of concept regarding the development of a biocompatible polymer membrane capable of selectively removing amyloid beta peptide from the blood and consequently from the cerebrospinal fluid.

**Keywords:** Amyloid beta peptide, Alzheimer's disease, Imprinted membranes, Poly(ethylene-co-vinyl alcohol)

## Introduction

The amyloidoses include a large number of degenerative disorders, that may be acquired or inherited, and which are characterized by a conformational change of a protein that is not correctly assembled by the cell. The anomalous protein accumulates in the tissue leading to an insoluble deposit that eludes the enzyme degradation involved in the normal remodeling process (1). Experimental evidence shows how the misfolding is correlated to changes in the surrounding environment such as oxidative stress and changes in pH or in the homeostasis of ions as occurs during the aging process (senile systemic amyloidosis). From a biochemical point of view, amyloid deposits consist of a precursor of abnormal fibrillar protein that constitutes the component that can be deposited at the level of a specific organ or distributed at the systemic

level involving various organs, by a serum nonfibrillar component serum amyloid P (SAP) and glycosaminoglycans (GAGs) that bind protein components.

Amyloid deposits are the basis of rare and serious diseases that have a huge social impact and are a challenge for physicians, also from the diagnostic point of view due to their diversity of distribution. At least 27 different types of amyloidosis are recognized and classified on the basis of the specific protein that forms the amyloid fibrils *in vivo* (2, 3). In particular, Alzheimer's disease is a neurodegenerative disease caused by fibrillar deposits, mainly located in the frontal and parietal lobes, containing a small peptide fragment of 39-42 amino acids derived from alteration of the proteolysis process of amyloid precursor protein. Although Alzheimer's disease is the most common form of neurodegenerative dementia, with over 26 million people affected to date worldwide, there is no treatment that can interrupt the progression of the disease or enable healing in the patient.

Recent studies have shown that administration of specific drugs can reduce brain amyloid protein deposits and preserve organ function. Vaccination against amyloid beta peptide is currently the most widely pursued strategy, even if an autoimmune response remains the main risk for affected patients. The use of secretases, benzodiazepines, sulfonamides, benzocaprolactams and recently statins represents the therapeutic approaches to reducing the formation of amyloid beta plaques (4). Changes in concentrations of amyloid beta protein peptide

Accepted: April 30, 2015

Published online: April 5, 2016

## Corresponding author:

Dr. Caterina Cristallini  
Istituto per i Polimeri Compositi e Biomateriali del CNR  
Sezione di Pisa  
Via Diotallevi, 2  
I-56126 Pisa, Italy  
c.cristallini@diccism.unipi.it

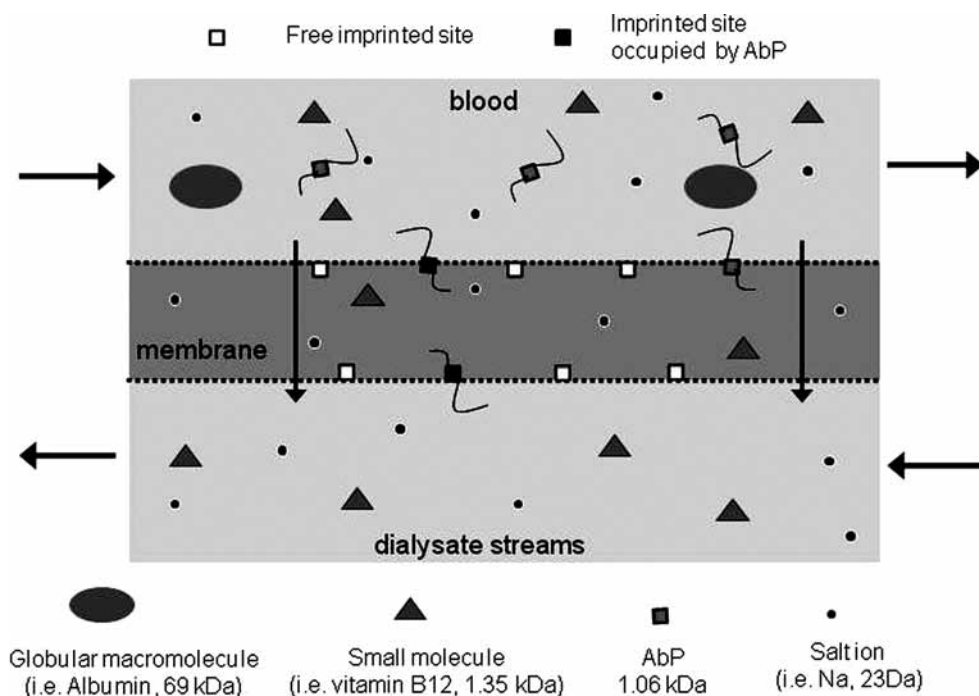


**Fig. 1** - Schema of scientific strategy for amyloid beta protein fragment 25-35 (AbP)-imprinted membranes used in dialyzer.

in body fluids are the earliest alterations observed in Alzheimer's disease (5). Some studies have shown that clinical improvement can be achieved by the mobilization of these peptides.

A significant number of therapeutic strategies are currently being examined, both in the laboratory and in clinical research, which aim to reduce the level of amyloid beta peptide (6). A peripheral treatment with gelsolin or GM1 at high affinity with amyloid beta peptide can reduce peptide content in the blood, leading to a reduction of the amyloid beta peptide levels in the brain (7). However, this treatment has been shown to not be suitable for long-term administration. A recent development is to provide a combination of an agent for sequestration of amyloid beta in the blood, with an apheresis device in contact with the blood which has receptors that bind the amyloid beta precursor protein (8).

The present study was based on the assumption that a removal device for protein amyloid peptides, through an extracorporeal purification system, might represent a feasible and complementary strategy for the treatment of patients suffering from neurodegenerative disease. The innovation of the proposed system consists in the modification of the device so that contact with the blood occurs at molecularly imprinted sites instead of biological receptors in order to avoid any severe autoimmune complications.

Generally, a dialyzer is designed to transfer solutes and water in a controlled way across a semipermeable membrane separating flowing blood and dialysate streams. The dialyzer allows removal of various toxins by diffusion, and/or in high-flux filters, by convection/filtration. The membranes, in the form of flat sheets or hollow fibers, enable the removal of molecules below the size of albumin (9).

In the approach proposed here, we designed a membrane that did not act as a simple filter based on pore dimension but instead specifically adsorbed the peptide involved in

Alzheimer's disease (Fig. 1). Our system could represent an alternative or complementary approach, based on a molecular-imprinting technique, offering a series of advantages including physical and chemical stability of imprinted membranes, good reusability, ease of sterilization and low cost.

The first step was the identification of suitable materials and technologies to realize this specific device. The selected material was poly(ethylene-co-vinyl alcohol) (EVAL) because it has already demonstrated high hemocompatibility (10), suitability for dialyzer production (11, 12) and ability to recognize, through a molecular-imprinting approach, protein molecules such as albumin and amylase (13, 14). Concerning the technology used for the creation of membranes, our efforts were directed toward a combination of phase inversion and molecular-imprinting techniques (15).

In this study we used as template the amyloid beta peptide sequence (i.e., 25-35), which represents the most toxic segment of the amyloid protein. Furthermore, to increase the capacity for recognition of the membrane toward the template, we developed a method of functionalization of the polymer chain using succinic anhydride (SA) (16). The aim was to decorate the membrane surface with carboxylic groups that, as is well known, are more effective with respect to hydroxyl groups in favoring molecular recognition at the level of active sites.

The peptide-imprinted membranes, both functionalized with SA and not, were examined from physicochemical, morphological, mechanical and functional points of view.

## Materials and methods

### Materials

EVAL (Solvay, Italy) with an ethylene molar content of 44% was used for the preparation of membranes. The solvents

used were dimethyl sulfoxide (DMSO, ACS purity degree; Carlo Erba Reagenti, Italy) and Milli-Q water (Millipore). SA (Sigma-Aldrich) was used for the chemical functionalization of EVAL. Gly-Ser-Asn-Lys-Gly-Ala-Ile-Ile-Gly-Leu-Met (AbP, molecular weight [Mw] = 1,060.27 Da; Sigma-Aldrich) was used as template, and Arg-Gly-Asp-Ser-Pro-Ala-Ser-Ser-Lys-Pro (Mw = 1,001.0 Da; Sigma-Aldrich) was used as analogue for the selectivity test.

### Membrane preparation

A first series of membranes (MIP1) was prepared by the phase inversion technique using pure EVAL. Solutions of EVAL (15% w/v) were obtained in DMSO under stirring at 60°C to obtain a complete dissolution of polymer. A prefixed amount of template was added to the solution after lowering the temperature to 37°C. The viscous blend was laid on a glass support to obtain a constant thickness using a knife machine (Separem Type SP) and dipped in a first phase inversion bath containing DMSO/H<sub>2</sub>O 50:50 solution. After 1 hour, the membranes were introduced into a second aqueous phase inversion bath for 24 hours and then subjected to a lyophilization procedure. For the preparation of the second series of membranes, a predefined amount of SA (2% in weight relative to the polymer content) was added to the initial DMSO solution, and then the same procedure used for MIP1 was followed to obtain functionalized and imprinted membranes (MIP2). Nonimprinted control membranes (CP1 and CP2) were prepared as previously described, without the addition of peptide template during the preparation. Template was extracted from MIP1 and MIP2 by repeated washing with aqueous solutions under dynamic conditions for 24 hours.

### Characterization

The morphology of membranes was analyzed by scanning electron microscopy (SEM; Jeol JSM 5600, Japan); freeze-dried membranes were sputtered with gold and observed at 20 kV. Chemical analysis was carried out by Fourier transform infrared (FTIR) chemical imaging (Perkin Elmer Spotlight 300, USA); the attenuated total reflectance (μATR) sampling technique was performed on samples of membranes (spectral resolution was 4 cm<sup>-1</sup>, spatial resolution was 100 × 100 μm), the use of FTIR allowed the evaluation of the distribution of components at the level of the membrane surface at different preparation steps, thus obtaining chemical and correlation maps to visualize their distribution and the efficacy of the molecular-imprinting procedure.

Template and analogous molecule dimensions after dissolution in water solution were evaluated by dynamic light scattering (DLS; Zetasizer Nano S, Malvern, UK).

Dynamic mechanical analysis (DMA) was performed (DMA8000; Perkin Elmer, USA) using a strain scan analysis to evaluate storage modulus (E') and loss modulus (E'') of membranes under dry conditions.

Rebinding and selectivity experiments were carried out by placing each membrane in an aqueous solution containing the peptide or analogue, respectively, at a concentration of 0.1 mg/mL at 37°C for 24 hours, to ensure the reaching of site saturation.

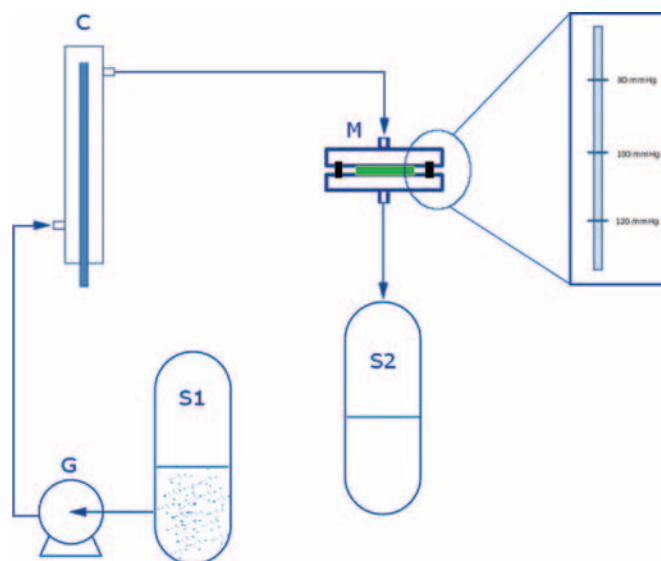


**Fig. 2** - Schematic representation of the experimental system used to test water permeability of the membranes under different transmembrane pressures. G = peristaltic pump; S1 = feed/refill tank; C = double jacket calibrated column; M = permeability cell containing membrane; S2 = recovery tank.

The solutions, after extraction, rebinding and selectivity tests, were analyzed by high-performance liquid chromatography (HPLC) using a C4 Prosphere HP Alltech column and UV detector (280 nm). A gradient elution was selected using internal mobile phase, starting from a volume ratio of Milli-Q-acetonitrile (modified by adding trifluoroacetic acid at 0.085% and 0.1% v/v, respectively) 30-70 (v/v) to 60-40 (v/v) at a constant rate of 1 ml/min for 20 minutes.

Hydraulic permeability was evaluated using the experimental apparatus described in Figure 2 by inducing a water flux through the membrane when subjected to an established pressure difference (transmembrane pressures TMP = 80, 100, 120 mmHg). One side of the membrane was subjected to a constant pressure, while the other side was maintained at atmospheric pressure. The water flux (Jv; cm<sup>3</sup> s<sup>-1</sup>) was measured by collecting the permeate water in a graduated tube. The value of water permeability Lp (cm s<sup>-1</sup> Pa<sup>-1</sup>) was evaluated as:

$$L_p = \frac{J_v}{TMPA} \text{ where } A \text{ is the membrane area.}$$

### Results

Figure 3 shows a schematic representation of possible interactions occurring at the molecular level among functional groups of copolymer chain and those of peptide amino acids. On the basis of pure EVAL, EVAL functionalized by SA and peptide sequence chemical structure, a large number of hydrogen bonds, both for MIP1 and MIP2, and electrostatic interactions, only in the case of MIP2, may occur with peptide groups.

In Figure 4, some representative results obtained by FTIR chemical imaging analysis for the membranes are reported. In the case of CP membranes, a series of characteristic

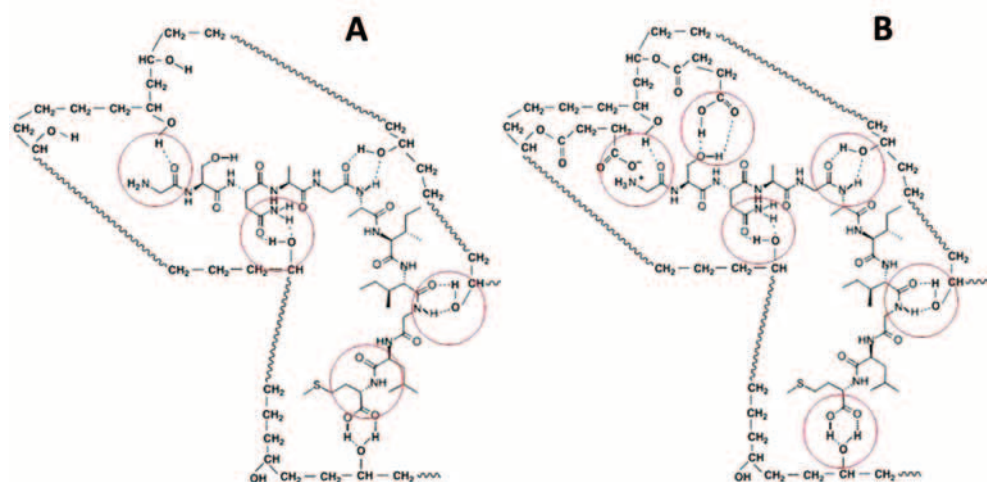


**Fig. 3** - Schematic representations of possible molecular interactions among functional groups of amyloid beta protein fragment 25-35 (AbP) and pure poly(ethylene-co-vinyl alcohol) (EVAL) (A) or succinic anhydride-modified EVAL (B) chemical structures.

absorptions of the copolymer chemical structure, including a wide band between 3,000 and 4,000  $\text{cm}^{-1}$  corresponding to OH-stretching, a peak between 3,000 and 2,700  $\text{cm}^{-1}$  relative to CHs stretching and another peak at 1,100  $\text{cm}^{-1}$  due to the presence of a C-OH bond, were identified (data not shown). By the overlapping of CP spectrum with peptide spectrum, the bands related to amide I and amide II at 1,668 and 1,632  $\text{cm}^{-1}$ , respectively, were evident. In the spectrum of MIP1 before template extraction (MIPT1), there is evident a small band at 1,650  $\text{cm}^{-1}$  relative to the presence of the peptide which moves to higher frequencies indicating the formation of interactions between matrix and peptide (Fig. 4A). Moreover, the map of correlations with respect to the average spectrum shows values close to 1, indicating a homogeneous distribution of the peptide on the sample surface (Fig. 4B); the same analysis carried out on a sample after template extraction (MIP1) shows a drastic reduction of the diagnostic band of the peptide, to confirm the effectiveness of the extraction procedure (Fig. 4C). The chemical map was performed both on MIP1 and on CP1 membranes after rebinding test and in both cases, the presence of peptide bands was detected, but the peak intensity for MIP was higher when compared with that of the control, pointing out how specific absorption predominated over the nonspecific (Fig. 4D).

The same study was performed also for the membranes after functionalization with SA. A significant result was the presence, on modified control membranes (i.e., CP2), of the peak at about 1,700  $\text{cm}^{-1}$  attributable to COOH group stretching. Also in the membranes before extraction (i.e., MIPT2), the presence of the peak corresponding to the peptide is evident (Fig. 4E), and the correlation map showed the peptide to be homogeneously distributed. After extraction there is evident a significant reduction of its intensity (Fig. 4F), while after rebinding, a small signal in the amide region appeared both on MIP2 and CP2. However, this signal was more intense in the MIP2 sample, indicating a specific absorption for the imprinted membrane.

In Figure 5, SEM images of membrane surfaces are shown. All of the series of membranes showed an asymmetric structure, the presence of a dense skin, which is known to be responsible for the selective properties and fingers (typical

structure of the phase inversion process). In addition, a microporosity uniformly distributed through the whole section of the samples was detected. Analogous results were obtained for the membranes modified by SA, which showed no substantial changes from a morphological point of view due to EVAL functionalization also in terms of microporosity, as shown by SEM images (Fig. 5E-H).

Further, the mechanical properties of the membranes were evaluated through DMA analysis. As shown in Figure 6, both MIP2 and CP2 showed a storage modulus ( $E'$ ) much greater than that registered for nonfunctionalized systems (MIP1, CP1). In contrast, no substantial difference due to imprinting method was observed, as can be seen from the comparison of  $E'$  for imprinted membranes (MIP1, MIP2) with their corresponding controls.

The results obtained by HPLC after extraction tests of the template are shown in Figure 7. Excellent removal of the peptide from nonfunctionalized membranes (close to 100%) was observed. In contrast, for those modified with SA, a slower and lower level of removal, even if quantitatively considerable, was detected; this confirms a high level of interaction of peptide and polymer in MIP2.

To evaluate the capability of imprinted membranes to specifically recognize the peptide, recognition tests introducing membranes in an aqueous peptide solution were carried out. SEM analysis performed on imprinted membranes before and after peptide rebinding did not show any evident change in the structure; a diffuse and homogeneous microporosity was retained (Fig. 5I, L). The results for imprinting performance are reported in Table I. The value of recognition factor for nonfunctionalized imprinted membranes, evaluated by HPLC analysis, was slightly higher than the unit, but in the case of membranes modified with SA, a higher value was detected.

Finally, to check whether the recognition sites were also selective, we performed a test of rebinding with a peptide analogue. Although the control membranes were able to bind a certain quantity of peptide due to microporosity and possible molecular interaction with the polymeric structure, the selectivity factors obtained for MIP1 and MIP2 were elevated (Tab. I).

In evaluating these systems for potential dialyzer use, some preliminary results regarding water permeability measured on



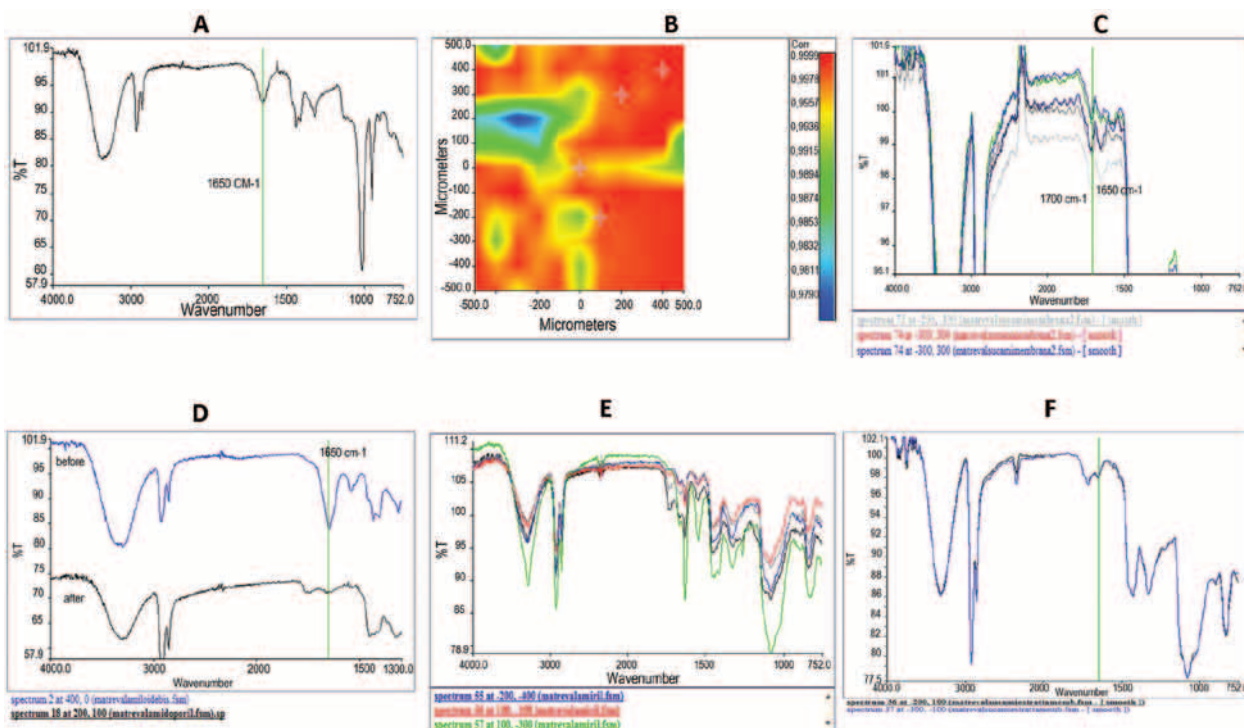


**Fig. 4** - Fourier transform infrared (FTIR): MIPT1 spectrum (A), correlation map of MIPT1 with respect to amyloid beta protein fragment 25-35 (Abp) amide I and amide II bands (B), MIP1 and MIPT1 comparison (median spectra) (C), MIP1 spectra after rebinding with peptide (D), MIPT2 spectra (E), and MIP2 spectrum (F).

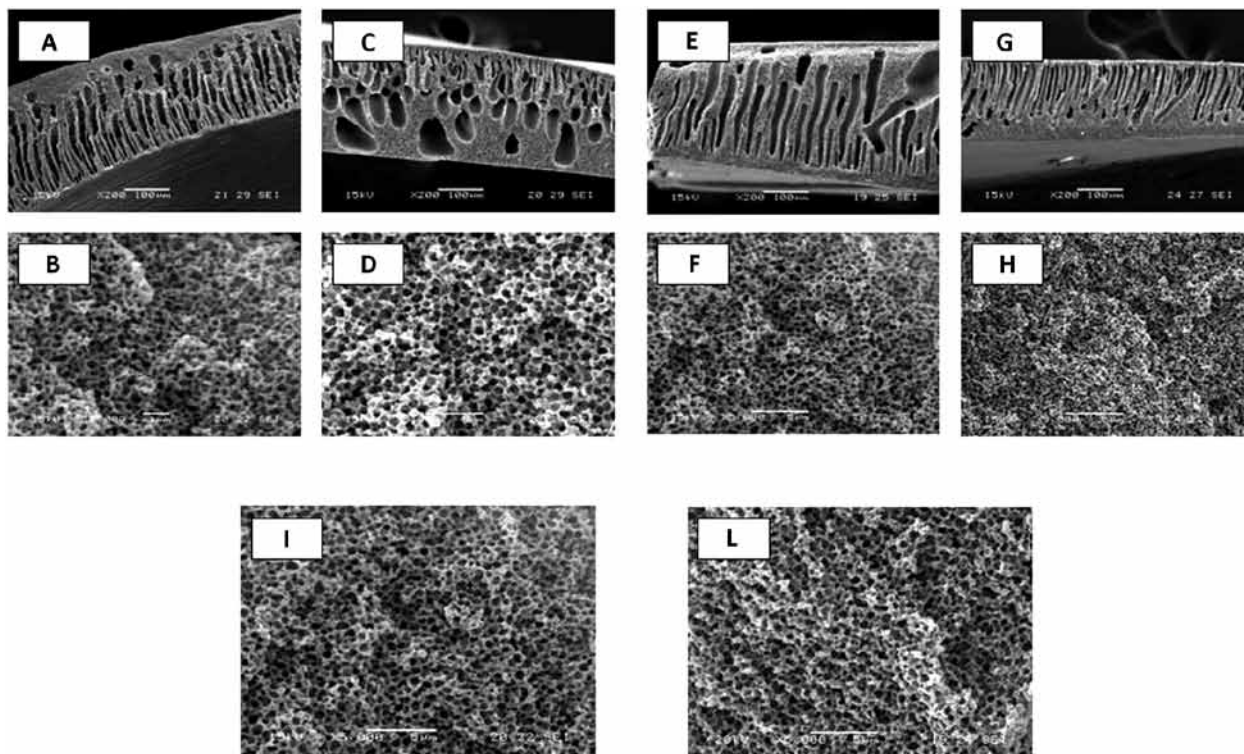


**Fig. 5** - Scanning electron microscopy images of cross-section of membranes: MIP1 (A), MIP1 microstructure (B), CP1 (C), CP1 microstructure (D), MIP2 (E), MIP2 microstructure (F), CP2 (G), CP2 microstructure (H), MIP2 microstructure before (I) and after Abp rebinding (L).

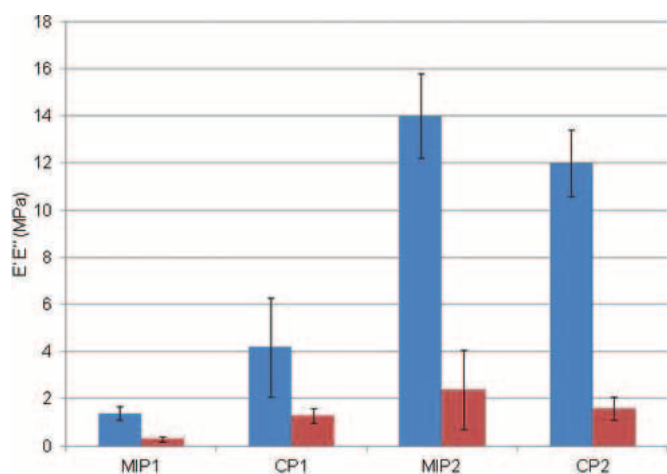


**Fig. 6** - Dynamic mechanical analysis (DMA): storage ( $E'$ ; blue bars) and loss ( $E''$ ; red bars) moduli for MIP1, MIP2, CP1 and CP2 membranes.

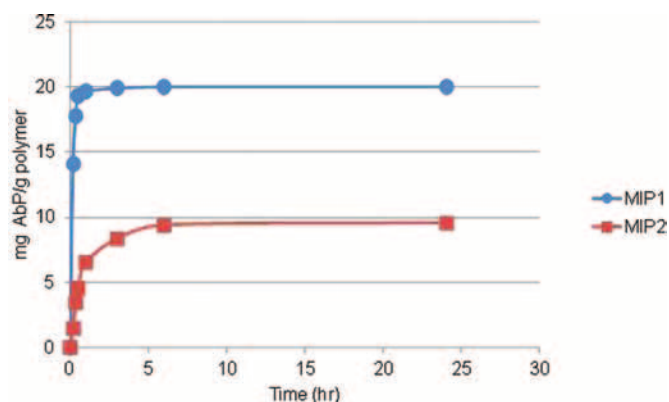


**Fig. 7** - High-performance liquid chromatography (HPLC) analysis: extraction kinetics of amyloid beta protein fragment 25-35 (AbP) from MIP1 and MIP2 membranes.

**TABLE I** - Recognition and selectivity tests for AbP-imprinted membranes and their respective control membranes in phosphate buffer solution

Membrane	Amount of AbP rebound ( $\text{mg}_{\text{template}}/\text{g}_{\text{polymer}}$ )	Amount of analogues rebound ( $\text{mg}_{\text{anal}}/\text{g}_{\text{polymer}}$ )	Recognition factor*	Selectivity factor†
MIP1	1.82	0.37	1.10	4.92
CP1	1.67	0.99		
MIP2	3.06	1.02	1.65	3.01
CP2	1.86	1.47		

AbP = amyloid beta protein fragment 25-35; CP = nonimprinted control membrane; CP1 = non modified membrane; CP2 = succinic anhydride-modified membrane; MIP = AbP-imprinted membrane; MIP1 = non modified imprinted membrane; MIP2 = succinic anhydride-modified imprinted membrane.

\* Recognition factor was calculated by dividing the amount of template rebound by MIP with the amount of template rebound by CP.

† Selectivity factor was calculated by dividing the amount of template rebound by the amount of analogues rebound.

**TABLE II** - Hydraulic permeability for the CP1 and CP2 membranes prepared in this study, also compared with commercial high-flux dialyzer membranes

Membrane	Transmembrane pressure	Hydraulic permeability ( $\text{cm s}^{-1} \text{Pa}^{-1}$ )			
		CP1	CP2	PS Fresenius*	PES Akzo*
$L_p \times 10^8$		4.5	3.23	2.9	10.5
$J_v \text{ cm s}^{-1} \times 10^3$	80 mm Hg	2.0	1.4		
	100 mm Hg	2.4	1.8		
	120 mm Hg	3.0	2.6		

CP1 = non modified poly(ethylene-co-vinyl alcohol) membrane; CP2 = succinic anhydride-modified poly(ethylene-co-vinyl alcohol) membrane; PS = polysulfone; PES = polyarylethersulphone.

\* The source for these data was (17).

CP1 and CP2 membranes were obtained using the experimental apparatus schematically shown in Figure 2. The results for water permeability are reported in Table II and compared with those of Fresenius and Akzo dialyzers. The  $L_p$  values were consistent with those of commercial high-flux dialyzer membranes (17).

## Discussion

This study allowed the production of EVAL-based membranes was carried out, using a combination of chemical functionalization and molecular imprinting technique for

selective removal of the amyloid beta protein peptide involved in Alzheimer's disease.

FTIR chemical imaging allowed the monitoring of the chemical composition of the membranes during the various stages of preparation, and provided the basis for a functional evaluation. This analysis demonstrated from a physicochemical point of view the efficacy of the preparation procedure to obtain peptide-imprinted membranes. In addition, the FTIR study of membranes modified by SA showed the presence of carboxylic groups, pointing to the success of the selected functionalization method.

The investigation by SEM enabled the evaluation of the morphology of the membranes obtained. A microporous and asymmetric structure and no modification of structure after template-rebinding render these membranes suitable for blood purification applications. Particularly interesting is the observation that the dimensions of membrane micropores were compatible with those of the peptide in solution, as shown by DLS measurements. The medium radius of the template in solution was  $324 \pm 15$  nm, while that of the analogue in solution was  $497 \pm 12$  nm.

This result is in accordance with the interactions foreseen on the basis of the chemical model; the interactions tended to arrange the peptide chain in a sort of niche formed by the polymer chains, increasing the possibility that the peptide could be retained inside the micropores of the membranes favoring its absorption.

DMA analysis showed an evident effect due to chemical modification through SA on the mechanical properties of the membranes, as observed by the increase of elastic modulus values measured for functionalized membranes. In contrast, the molecular-imprinting procedure did not seem to alter the mechanical properties of polymeric membranes.

Concerning the HPLC results, the analysis of template extraction confirmed a greater interaction between peptide and polymer in MIP2. The recognition and selectivity factors reflected the capability of both imprinted membranes of rebinding the selected peptide in a specific and selective manner. In this respect, it can be hypothesized that the increase of the rigidity of the membranes after functionalization could elicit a higher conformational stability to the active and complementary sites, thus increasing the performance of membranes in terms of molecular recognition.

Concerning selectivity behavior, although high selectivity factors were found for both imprinted membranes, the presence of carboxylic groups on the functionalized membrane surface would induce an increase of molecular interaction with the analogue peptide after rebinding. The differences in the amino acid sequence of the 2 peptides – in particular, the presence of serine (in high numbers) and lysine in the analogue structure – could explain the higher affinity of the analogue for the functionalized membranes, with respect to the template after rebinding, thus leading to a lower selectivity factor for MIP2 than MIP1.

The high selectivity factors measured for MIP1 and MIP2 are particularly significant considering the close similarity between the template and analogue in terms of chemical structure (amino acid sequences), molecular weight and molecular size of peptide.

The preliminary results for hydraulic permeability obtained for EVAL-based membranes encourage us to continue the study of these systems, evaluating solute permeability and the effect of imprinting procedure on the transport properties of the imprinted membrane.

The positive results, even if preliminary, obtained in this study can be considered a viable proof of concept toward developing a device able to rebind and thus remove the amyloid beta protein peptide. The next steps will be a further exploration of kinetic studies using different template concentrations and the determination of adsorption isotherms. A better understanding of the factors involved in the misfolding mechanism will allow the evaluation of the use of other markers (i.e., tau) of neuropathology in cerebrospinal fluid and in blood, to be used in diagnostic and/or therapeutic methods (18, 19). Despite the fact that the achievement of an effective treatment for this complex pathology is still far from being realized, there is an urgent scientific interest in identifying preventative treatments and diagnostic tools. In this context, the use of molecularly imprinted membranes for the markers involved in Alzheimer's disease, proposed for the first time in this work, can be considered an interesting and versatile strategy that unites the main efforts being made toward achieving concrete results.

Further, solute permeability measurements, hemocompatibility tests and dynamic peptide removal in body fluids are currently under careful investigation.

## Acknowledgment

The authors would like to acknowledge Dr. C. Mura and Dr. L. Fasciani for their helpful technical support.

## Disclosures

Financial support: This work was supported by Institutional funds of CNR.

Conflict of interest: The authors declare no conflict of interest.

Meeting presentation: Data have been presented at the SIB National Congress, 2-4 July 2014, Palermo, Italy.

## References

1. Hirschfield GM, Hawkins PN. Amyloidosis: new strategies for treatment. *Int J Biochem Cell Biol.* 2003;35(12):1608-1613.
2. Zhou L, Chan KH, Chu LW, et al. Plasma amyloid- $\beta$  oligomers level is a biomarker for Alzheimer's disease diagnosis. *Biochem Biophys Res Commun.* 2012;423(4):697-702.
3. Tan SY, Pepys MB, Hawkins PN. Treatment of amyloidosis. *Am J Kidney Dis.* 1995;26(2):267-285.
4. Selkoe DJ. Alzheimer's disease: genes, proteins, and therapy. *Physiol Rev.* 2001;81(2):741-766.
5. Zimmermann R, Huber E, Schamber C, et al. Plasma concentrations of the amyloid- $\beta$  peptides in young volunteers: the influence of the APOE genotype. *J Alzheimers Dis.* 2014;40(4):1055-1060.
6. Wolfe MS. Therapeutic strategies for Alzheimer's disease. *Nat Rev Drug Discov.* 2002;1(11):859-866.
7. Matsuoka Y, Saito M, LaFrancois J, et al. Novel therapeutic approach for the treatment of Alzheimer's disease by peripheral administration of agents with an affinity to beta-amyloid. *J Neurosci.* 2003;23(1):29-33.

8. Mattner F, Schmidt W. Methods of treating Alzheimer's disease with an apheresis device. US Patent 7,935,252B2. 2001. Issued May 3, 2011.
9. Stegmayr BG. A survey of blood purification techniques. *Transfus Apheresis Sci.* 2005;32(2):209-220.
10. Lelli L, Guerra GD, Lazzeri L, Barbani N, Bonaretti A, Giusti P. Blood-compatible polymers and their characterization: a simple sensitive assay for hemocompatibility evaluation. *Int J Polymer Analysis Characterization.* 1995;1(2):131-136.
11. Sakai K. Determination of pore size and pore size distribution 2. Dialysis membranes. *J Membr Sci.* 1994;96:91-130.
12. Avramescu ME, Sager WFC, Mulder MHV, Wessling M. Preparation of ethylene vinylalcohol copolymer membranes suitable for ligand coupling in affinity separation. *J Membr Sci.* 2002;210(1):155-173.
13. Silvestri D, Cristallini C, Ciardelli G, Giusti P, Barbani N. Molecularly imprinted bioartificial membranes for the selective recognition of biological molecules. Part 2: release of components and thermal analysis. *J Biomater Sci Polym Ed.* 2005;16(3):397-410.
14. Lee MH, Thomas JL, Tasi SB, Liu B-D, Lin HY. Formation and recognition characteristics of albumin-imprinted poly(ethylene-co-vinyl-alcohol) membranes. *J Nanosci Nanotechnol.* 2009;9(6):3469-3477.
15. Guerra GD, Barbani N, Coluccio ML, Cristallini C. Cross-linked ionomeric materials from poly(styrene-alt-maleic anhydride) and poly(ethylene glycol) for biomedical applications: a preliminary investigation. *J Appl Biomater Biomech.* 2006;4(2):97-101.
16. Wüpper A, Dellanna F, Baldamus CA, Woermann D. Local transport processes in high-flux hollow fiber dialyzer. *J Membr Sci.* 1997;131(1-2):181-193.
17. Blennow K, Hampel H. CSF markers for incipient Alzheimer's disease. *Lancet Neurol.* 2003;2(10):605-613.
18. Bates KA, Verdile G, Li Q-X, et al. Clearance mechanisms of Alzheimer's amyloid- $\beta$  peptide: implications for therapeutic design and diagnostic tests. *Mol Psychiatry.* 2009;14(5):469-486.
19. Pláteník J, Fišar Z, Buchal R, et al. GSK3 $\beta$ , CREB, and BDNF in peripheral blood of patients with Alzheimer's disease and depression. *Prog Neuropsychopharmacol Biol Psychiatry.* 2014;50: 83-93.